



# CHORUS

This is the accepted manuscript made available via CHORUS. The article has been published as:

## Unexpected distribution of $\nu 1f_{7/2}$ strength in $^{49}\text{Ca}$

H. L. Crawford *et al.*

Phys. Rev. C **95**, 064317 — Published 21 June 2017

DOI: [10.1103/PhysRevC.95.064317](https://doi.org/10.1103/PhysRevC.95.064317)

# Unexpected distribution of $\nu 1f_{7/2}$ strength in $^{49}\text{Ca}$

H. L. Crawford<sup>1,2\*</sup>, A. O. Macchiavelli<sup>1</sup>, P. Fallon<sup>1</sup>, M. Albers<sup>3</sup>, V. M. Bader<sup>4,5</sup>, D. Bazin<sup>4</sup>, C. M. Campbell<sup>1</sup>, R. M. Clark<sup>1</sup>, M. Cromaz<sup>1</sup>, J. Dilling<sup>6,7</sup>, A. Gade<sup>4,5</sup>, A. Gallant<sup>6,7</sup>, J. D. Holt<sup>6</sup>, R. V. F. Janssens<sup>3</sup>, R. Krücken<sup>6,7</sup>, C. Langer<sup>4</sup>, T. Lauritsen<sup>3</sup>, I. Y. Lee<sup>1</sup>, J. Menéndez<sup>8</sup>, S. Noji<sup>4</sup>, S. Paschalis<sup>9,†</sup>, F. Recchia<sup>4</sup>, J. Rissanen<sup>1</sup>, A. Schwenk<sup>9,10</sup>, M. Scott<sup>4,5</sup>, J. Simonis<sup>9,10</sup>, S. R. Stroberg<sup>4,5,‡</sup>, J. A. Tostevin<sup>11</sup>, C. Walz<sup>9</sup>, D. Weisshaar<sup>4</sup>, A. Wiens<sup>1</sup>, K. Wimmer<sup>12,§</sup>, and S. Zhu<sup>3</sup>

<sup>1</sup>*Nuclear Science Division, Lawrence Berkeley National Laboratory, Berkeley, CA 94720, USA*

<sup>2</sup>*Institute for Nuclear and Particle Physics and Department of Physics and Astronomy, Ohio University, Athens, OH 45701, USA*

<sup>3</sup>*Physics Division, Argonne National Laboratory, Argonne, IL 60439, USA*

<sup>4</sup>*National Superconducting Cyclotron Laboratory,*

*Michigan State University, East Lansing, MI 48824, USA*

<sup>5</sup>*Department of Physics and Astronomy, Michigan State University, East Lansing, MI 48824, USA*

<sup>6</sup>*TRIUMF, 4004 Wesbrook Mall, Vancouver, British Columbia V6T 2A3, Canada*

<sup>7</sup>*Department of Physics and Astronomy, University of British Columbia, Vancouver, British Columbia V6T 1Z1, Canada*

<sup>8</sup>*Department of Physics, The University of Tokyo, Hongo, Bunkyo-ku, Tokyo 113-0033, Japan*

<sup>9</sup>*Institut für Kernphysik, Technische Universität Darmstadt, 64289 Darmstadt, Germany*

<sup>10</sup>*ExtreMe Matter Institute EMMI, GSI Helmholtzzentrum für Schwerionenforschung GmbH, 64291 Darmstadt, Germany*

<sup>11</sup>*Department of Physics, University of Surrey, Guildford, Surrey GU2 7XH, United Kingdom and*

<sup>12</sup>*Department of Physics, Central Michigan University, Mt. Pleasant, MI 48859, USA*

The calcium isotopes have emerged as a critical testing ground for new microscopically derived shell-model interactions, and a great deal of experimental and theoretical focus has been directed toward this region. We investigate the relative spectroscopic strengths associated with  $1f_{7/2}$  neutron hole states in  $^{47,49}\text{Ca}$  following one-neutron knockout reactions from  $^{48,50}\text{Ca}$ . The observed reduction of strength populating the  $7/2_1^-$  state in  $^{49}\text{Ca}$ , as compared to  $^{47}\text{Ca}$ , is inconsistent with shell-model calculations using both phenomenological interactions such as GXPF1, and interactions derived from microscopically-based two- and three-nucleon forces. The result suggests a fragmentation of the  $l=3$  strength to higher-lying states as suggested by the microscopic calculations, but the observed magnitude of the reduction is not reproduced in any shell-model description.

PACS numbers:

The calcium isotopic chain is a focus of nuclear structure physics, both from experimental and theoretical perspectives. This chain contains novel examples of evolving shell structure far from stability [1, 2] and is an active region to test three-body (3N) forces in microscopically derived shell-model interactions and large-space ab initio calculations [1, 3–16].

From the theoretical perspective, new developments are enabling a microscopic description of these nuclei, with calculations being performed from  $^{48}\text{Ca}$  to  $^{70}\text{Ca}$  using effective shell-model interactions [3, 10], or large-space calculations [4, 8, 9, 11, 13, 16] based on two-nucleon (NN) and 3N interactions derived from chiral effective field theory. These calculations have already shown differences compared to predictions of phe-

nomological shell-model interactions, even for nuclei as close to stability as  $^{50}\text{Ca}$ . For larger neutron number  $N$ , predictions for the location of the dripline are strongly model dependent, varying from  $^{60}\text{Ca}$  to  $^{76}\text{Ca}$  [3, 4, 17]. Data on the structure of the neutron-rich Ca isotopes is critical to benchmark the various new calculations and validate their predictions.

Measurements of properties such as masses [1, 5] and spectroscopy [2] at the limits of current facilities are well reproduced by the newest calculations, but recent data have revealed discrepancies with theoretical predictions, bringing into question extrapolations toward the dripline. For example, a laser spectroscopy measurement at CERN-ISOLDE [14] reported charge radii that show an anomalously large increase from  $^{48}\text{Ca}$  to  $^{52}\text{Ca}$ , significantly exceeding all theoretical predictions.

Single-particle occupancies, while not direct observables, can provide a test for theoretical descriptions. Phenomenological interactions like GXPF1 [18, 19] and microscopically based interactions both find reasonable agreement with spectroscopic data, but they predict different distributions of the neutron  $\nu 1f_{7/2}$  strength in  $^{49}\text{Ca}$ . Phenomenological models are more consistent with the single-particle description, where one would ex-

---

\*Corresponding author: hlcrawford@lbl.gov

†Present address: Department of Physics, University of York, York YO10 5DD, United Kingdom

‡Present address: TRIUMF, 4004 Wesbrook Mall, Vancouver, British Columbia V6T 2A3, Canada

§Present address: Department of Physics, The University of Tokyo, Hongo, Bunkyo-ku, Tokyo 113-0033, Japan.

pect the full  $\nu 1f_{7/2}$  strength to be concentrated in the  $7/2_1^-$  state for Ca nuclei at and immediately beyond  $N=28$ . However, the microscopic interactions suggest a possible fragmentation of this strength.

In this Letter, we report the results of an experiment using the high-resolution  $\gamma$ -ray array GREYINA [20] to measure exclusive neutron-knockout cross sections from  $^{50}\text{Ca}$  to states in  $^{49}\text{Ca}$ , and from  $^{48}\text{Ca}$  to  $^{47}\text{Ca}$ . Based on the data and theoretical cross sections, calculated under the assumption of the sudden removal of a neutron with a given set of quantum numbers [21, 22], we extract spectroscopic factors, that can be compared with the predictions of shell-model calculations. A relative measurement, such as that performed here comparing  $^{48}\text{Ca}(-1n)$  and  $^{50}\text{Ca}(-1n)$  neutron removal, provides a framework to firmly establish the trend in the spectroscopic strength distributions for the neutron  $pf$  orbitals. Our results indicate a decrease in the population of the lowest  $7/2^-$  state in  $^{50}\text{Ca}$ , at odds with the phenomenological description. This trend is partially reproduced by NN+3N calculations in the  $pf$  shell-model space.

The experiment was performed at the National Superconducting Cyclotron Laboratory (NSCL) at Michigan State University. Secondary beams of  $^{48,50}\text{Ca}$  were produced following fragmentation of a 140-MeV/u  $^{82}\text{Se}$  primary beam on a 423 mg/cm<sup>2</sup>  $^9\text{Be}$  target. Reaction products were separated through the A1900 fragment separator [23], based on magnetic rigidity and relative energy loss through a 600 mg/cm<sup>2</sup> Al degrader wedge. Fragments were delivered with a momentum acceptance of 2%  $\Delta p/p$  and impinged on a 370 mg/cm<sup>2</sup>-thick Be target at the target position of the S800 spectrograph [24]. The knockout products were identified event-by-event through time-of-flight and energy loss measured by the focal plane detectors of the S800.

Seven GREYINA modules surrounded the target position of the S800 to detect  $\gamma$  rays emitted from excited states populated in the knockout residues. Four modules were placed at  $\theta \sim 58^\circ$ , and three at  $\theta \sim 90^\circ$  relative to the beam direction. The  $\gamma$ -ray interaction position information from GREYINA, along with the particle trajectory information from the S800 were used to provide an accurate event-by-event Doppler reconstruction of the observed  $\gamma$  rays, achieving a  $\gamma$ -ray resolution of 1.5%. Yields for individual transitions were determined by a fit to data using a GEANT4 simulation of the GREYINA response [30], including the angular distribution of emitted  $\gamma$  rays (based on the calculated population of the  $m$  substates in the knockout reaction); the simulation is conservatively taken to contribute an absolute error of 1%. The results are summarized in Fig. 1 and Table I.

The Doppler-shift corrected spectra of  $\gamma$ -rays in coincidence with  $^{47,49}\text{Ca}$  reaction products are presented in Figs. 1(a) and (b). The corresponding level and decay schemes, as observed in this work, are shown in

Figs. 1(c) and (d). Thirteen transitions are observed and associated with levels in  $^{47}\text{Ca}$  populated in the one neutron removal reaction. The majority of the transitions were previously observed [26] and their placement in the level scheme follows the literature. Two  $\gamma$  rays, at 3425 and 3267 keV were not previously reported, but are placed as transitions directly to the ground state, supported by  $\beta$ -decay data [27]. Where statistics are sufficient, the level scheme was verified by  $\gamma$ - $\gamma$  coincidences. For  $^{48}\text{Ca}(-1n)$ , the states of primary interest are at 2.60, 2.58 and 0 MeV (ground state) corresponding to direct removal of a  $s_{1/2}$ ,  $d_{3/2}$  and  $f_{7/2}$  neutron, respectively.

For  $^{49}\text{Ca}$ , eight transitions of appreciable statistics, all previously placed in the level scheme, are observed [28, 29]. The 3.36 MeV state and the ground state are of primary interest, corresponding predominantly to the removal of a  $f_{7/2}$  and  $p_{3/2}$  neutron, respectively. Recent work has also suggested that the  $7/2_1^-$  state has wavefunction components from the coupling of  $p_{3/2}$  neutron to the  $2_1^+$  state in  $^{48}\text{Ca}$  [30], though we do not expect to populate this state through this component of the wavefunction. We note that the  $1/2^-$  state at 2.02 MeV may also be populated through direct removal of a  $p_{1/2}$  neutron, should such a configuration be present in the  $^{50}\text{Ca}$  ground state.

Cross sections for the population of the states of interest in  $^{47,49}\text{Ca}$  via direct -1n knockout are given in Table I and were deduced from the observed level schemes while accounting for feeding from higher-lying states. Cross sections were corrected for losses associated with the momentum acceptance of the S800. The exclusive parallel momentum distributions were found to be consistent with the expected angular momentum transfer for these states; i.e.,  $l = 0, 2$ , and 3 for the 2.60, 2.58 MeV, and ground state, respectively, in the  $^{48}\text{Ca}(-1n)$  reaction and  $l = 3$  and 1 for the 3.36 MeV and ground state in the  $^{50}\text{Ca}(-1n)$  reaction (see Fig. 1(e) and (f)). A fit of the partial momentum distributions with the calculated distributions allowed us to deduce the required acceptance correction factors, on average contributing a correction of order 10%, with a maximum value of 20%. These corrections contributed an error of 10% to the overall error budget. This procedure also ensured that any population of states via an indirect reaction process, as identified by a momentum distribution shifted to lower momentum [31], was not included in the calculation of spectroscopic factors. Such indirect population accounts predominantly for the population of higher-energy states in the -1n removal.

The measured direct neutron knockout cross sections can be compared to theoretical predictions. To do this we relate the measured cross section to a theoretical single-particle knockout cross section,  $\sigma_{sp}$ , for removal of a neutron in an orbit  $nlj$  assuming a spectroscopic factor,  $C^2S = 1$ . The formalism and methodology to

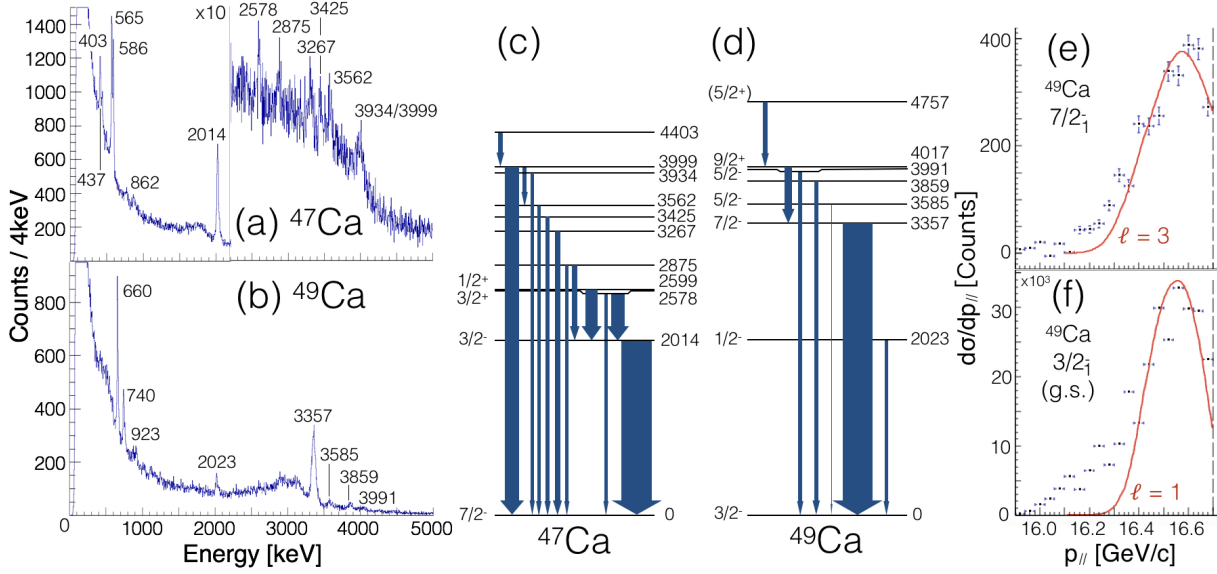


FIG. 1: Experimentally observed  $\gamma$ -ray spectra (left) and populated level schemes (right) of (a)  $^{47}\text{Ca}$  from  $^{48}\text{Ca}(-1n)$ , and (b)  $^{49}\text{Ca}$  from  $^{50}\text{Ca}(-1n)$  reactions. Experimental spectra are marked with the observed transitions in keV. In (c) and (d) the assigned spins and parities come from the literature, while the width of the arrows corresponds to the (efficiency-corrected) relative intensity of the  $\gamma$ -ray transitions. For reference,  $S_n(^{47}\text{Ca}) = 7.3$  MeV and  $S_n(^{49}\text{Ca}) = 5.1$  MeV. (e) and (f) show the parallel momentum distributions for the  $7/2^-_1$  and  $3/2^-_1$  states in  $^{49}\text{Ca}$  respectively, showing direct contributions and tails to low momentum resulting from indirect reaction processes.

calculate  $\sigma_{sp}$  are given in Refs. [21, 22, 32]. From the calculated  $\sigma_{sp}$  and measured cross sections,  $\sigma_{-1n}$  in Table I we extract experimental spectroscopic factors  $C^2S_{exp}$ .

To compare with shell-model calculations, we correct by  $R_S$ , a suppression or quenching factor, required to scale calculated single-particle cross sections to measurements [21, 32]. Following Ref. [31], the  $R_S$  values used here and given in Table I were obtained from a fit to the systematics of  $R_S$  as a function of  $\Delta S = S_n - S_p$  for inclusive neutron knockout data [21]. A 20% systematic error associated with the local scatter in  $R_S$  as a function of  $\Delta S$  is propagated in the calculation of  $C^2S_{exp}^{norm}$ .

The value of  $C^2S_{exp}^{norm} = 9.3(^{+1.2}_{-1.3})_{stat}(\pm 1.9)_{sys}$  for the lowest  $1f_{7/2}$  state in  $^{47}\text{Ca}$  is consistent with the results obtained in (p, d) and (d, t) neutron transfer measurements [33, 34] and with the expected value of 8 (i.e., a full  $1f_{7/2}$  orbital in the  $^{48}\text{Ca}$  ground state). The spectroscopic factors to the lowest  $1d_{3/2}$  state at 2.58 MeV and the lowest  $2s_{1/2}$  state at 2.60 MeV in  $^{48}\text{Ca}(-1n)$  are similarly consistent with the literature values. However, in  $^{50}\text{Ca}(-1n)$  the spectroscopic factor to the first  $7/2^-$  state at 3.36 MeV is significantly lower than that observed in  $^{48}\text{Ca}(-1n)$ , at only  $4.7(^{+0.6}_{-0.4})_{stat}(\pm 0.9)_{sys}$ . The  $C^2S_{exp}^{norm}$  values for the population of the ground state ( $\nu 2p_{3/2}^1$  level) in  $^{49}\text{Ca}$ , and the first excited state at 2.02 MeV ( $\nu 2p_{1/2}^1$  state) are  $2.7(\pm 0.4)_{stat}(\pm 0.5)_{sys}$  and  $0.4(\pm 0.1)_{stat}(\pm 0.1)_{sys}$ , respectively.

We updated the calculations of Refs. [3, 6, 10] to com-

pare with these new experimental measurements. Following the same perturbative many-body approach for generating the  $pf$  and  $pf g_{9/2}$  valence-space Hamiltonians outlined in Ref. [10], we start from NN+3N interactions that predict realistic saturation properties of nuclear matter within theoretical uncertainties [35, 36]. These interactions have also been used to study the Ca isotopes [13, 14]. By varying the low-resolution cutoff in NN forces,  $\lambda_{NN} = 1.8 - 2.2 \text{ fm}^{-1}$ , we obtain an uncertainty estimate for the calculations. Low-lying excited states for the  $pf$ -shell calculation agree reasonably well with experiment. For instance in  $^{47}\text{Ca}$ , the  $3/2^-_1$  and  $7/2^-_2$  states lie at 2.15 MeV and 3.23 MeV excitation energy, respectively, for  $\lambda_{NN} = 1.8 \text{ fm}^{-1}$ , within 200 keV of experiment, and  $1/2^-_1$  and  $3/2^-_2$  states are predicted below 3 MeV, in agreement with spin-unassigned experimental levels. All states are shifted 300 keV and 600 keV higher in energy for  $\lambda_{NN} = 2.0, 2.2 \text{ fm}^{-1}$ . In  $^{49}\text{Ca}$  the central energy values given by  $\lambda_{NN} = 2.0 \text{ fm}^{-1}$  of  $E(1/2^-_1) = 2.07(05) \text{ MeV}$ ,  $E(5/2^-_1) = 2.32(03) \text{ MeV}$ ,  $E(7/2^-_1) = 3.40(30) \text{ MeV}$ , and  $E(5/2^-_2) = 3.53(25) \text{ MeV}$ , with approximate uncertainties in parentheses, agree well with experiment, outside of the  $5/2^-_1$  state which is predicted more than 1 MeV too low in energy.

The ratio of spectroscopic factors to populate the lowest  $7/2^-_1$  state in the neutron knockout from  $^{50}\text{Ca}$  and  $^{48}\text{Ca}$  is plotted in Fig. 2. There is marked difference between the experimental and theoretical ratios. In the phenomenological description, the full  $1f_{7/2}$  strength of

TABLE I: Summary of states populated in direct one-neutron removal reactions from  $^{48}\text{Ca}$  and  $^{50}\text{Ca}$ . Level energies and spin/parity assignments are from [26, 28, 29]. Single-particle theoretical cross-sections,  $\sigma_{sp}$ , along with an  $A$ -dependent center-of-mass correction [37] are used to deduce the values for  $\text{C}^2\text{S}_{exp}$ .  $R_S$  quenching factors used to calculate  $\text{C}^2\text{S}_{exp}^{norm}$  are extracted based on [21]. Theoretical values are provided for the phenomenological GXPF1 shell-model interaction, as well as the NN+3N-based interaction in the  $pf$  and  $pf_{g_{9/2}}$  model spaces. The range of values for the NN+3N cases is an estimate for the uncertainty associated with varying the NN cutoff in the derivation of the interaction. The inclusive cross sections for the neutron removal channel in each case are also shown.

Level Energy [keV]	$J^\pi$	$\sigma_{-1n}$ [mb]	$\sigma_{sp}$ [mb]	$\text{C}^2\text{S}_{exp}$	$R_S$	$\text{C}^2\text{S}_{exp}^{norm}$	Theoretical $\text{C}^2\text{S}$			
							GXPF1	$pf$	NN+3N	$pf_{g_{9/2}}$
$^{48}\text{Ca} \rightarrow ^{47}\text{Ca}$										
0	$7/2^-$	$70.6_{-9.6}^{+8.4}$	11.01	$6.4_{-0.9}^{+0.8}$	0.69	$9.3_{(-1.3)}^{(+1.1)}_{stat}(\pm 1.9)_{sys}$	7.7	7.2 – 7.4	6.7 – 7.0	
2014	$3/2^-$	$\leq 1.4$	11.24	$\leq 0.1$	0.66	$\leq 0.2$	0.06	0.05 – 0.07	0.05 – 0.07	
2578	$3/2^+$	$9.4_{-1.9}^{+3.1}$	7.46	$1.3_{-0.3}^{+0.4}$	0.65	$1.9_{(-0.4)}^{(+0.6)}_{stat}(\pm 0.4)_{sys}$				
2599	$1/2^+$	$10.5_{-1.3}^{+1.4}$	12.58	0.8(1)	0.65	$1.3(\pm 0.2)_{stat}(\pm 0.2)_{sys}$				
Direct Inclusive: 111(10) [ <i>Total inclusive:</i> 123(10)]										
$^{50}\text{Ca} \rightarrow ^{49}\text{Ca}$										
0	$3/2^-$	$41.8_{-5.9}^{+5.2}$	18.63	2.1(3)	0.77	$2.7_{(-0.4)}^{(+0.3)}_{stat}(\pm 0.5)_{sys}$	1.73	1.70 – 1.72	1.50 – 1.56	
2023	$1/2^-$	$4.4_{-0.5}^{+0.8}$	15.04	$0.28_{-0.03}^{+0.05}$	0.74	$0.37_{(-0.05)}^{(+0.07)}_{stat}(\pm 0.1)_{sys}$	0.17	0.12 – 0.14	0.12 – 0.14	
3357	$7/2^-$	$38.9_{-3.9}^{+5.1}$	10.87	$3.4_{-0.3}^{+0.4}$	0.72	$4.7_{(-0.5)}^{(+0.6)}_{stat}(\pm 0.9)_{sys}$	7.7	5.6 – 5.7	6.3 – 6.7	
3750 - 3900 <sup>a</sup>	$7/2^-$	–	–	–	–	–	–	1.5 – 1.8	0.4 – 0.5	
4017	$9/2^+$	$\leq 0.8$	11.39	$\leq 0.07$	0.71	$\leq 0.09$	–	–	0.15 – 0.20	
Direct Inclusive: 98(10) [ <i>Total inclusive:</i> 116(10)]										

<sup>a</sup>Prediction for  $7/2_2^-$  state in NN + 3N calculations; range captures the prediction for calculations in the  $pf$  model space (400 keV above  $7/2_1^-$ ) and  $pf_{g_{9/2}}$  model space (550 keV above  $7/2_1^-$ ).

$\text{C}^2\text{S} = 8$  is concentrated in the lowest  $7/2^-$  state in both the  $^{48}\text{Ca}$  and  $^{50}\text{Ca}$  reactions. For the NN+3N calculations, the  $1f_{7/2}$  strength is also largely concentrated in the  $7/2_1^-$  state at  $N=28$ , but in  $^{50}\text{Ca}(-1n)$ , a reduced strength to the  $7/2_1^-$  state is seen, particularly for the  $pf$  valence-space calculation. Consequently, both GXPF1 and the  $pf_{g_{9/2}}$ NN+3N interaction predict a ratio  $\approx 1$ , while for the  $pf$  interaction the ratio is 0.78. Experimentally, we determine a ratio of  $0.51(\pm 0.09)_{stat}(\pm 0.15)_{sys}$ , shown by the blue bar in Fig. 2. The error bar indicates the statistical error from the data; the bracketed error bar includes the systematic error from the determination of  $R_S$ .

The disagreement with the well-established phenomenological GXPF1 interaction can provide important feedback to refine this family of interactions. Likewise, disagreement with the  $pf_{g_{9/2}}$  NN+3N predictions along with deficiencies in spectroscopy of low-lying  $9/2^+$  states [28, 38] may call for an improved treatment in valence spaces beyond one major shell [39]. The most reasonable agreement is found for the the  $pf$  NN+3N interaction, in which the reduced cross section in the  $^{50}\text{Ca}(-1n)$  reaction is due to a fragmentation of the  $1f_{7/2}$  strength to states at higher excitation energies in  $^{49}\text{Ca}$ . However, we see no evidence of significant population to a higher-lying candidate  $7/2_2^-$  state (within a detection limit of approximately 3 mb, assuming de-excitation directly to the ground state). It is also worth noting

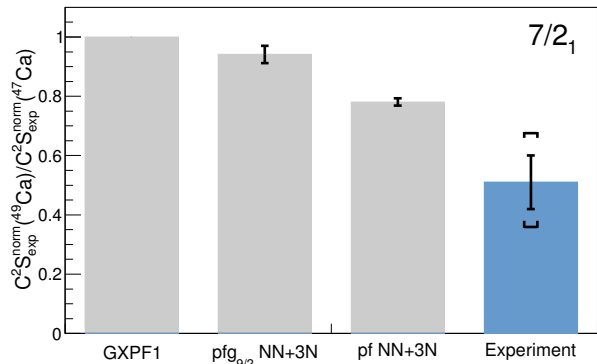


FIG. 2: Ratio of the spectroscopic factor for the population of the first  $7/2^-$  state in one-neutron knockout from  $^{50}\text{Ca} \rightarrow ^{49}\text{Ca}$  /  $^{48}\text{Ca} \rightarrow ^{47}\text{Ca}$ , as predicted by the shell model calculations using the GXPF1A phenomenological interaction (left), NN+3N interaction in the  $pf$  (center right) and  $pf_{g_{9/2}}$  (center left) model spaces, and measured (blue column, right).

that the extent of the reduction is larger in experiment than the predictions of the  $pf$ -shell NN+3N calculation, despite the fact that these interactions are now in good agreement with experimental excitation spectra and electromagnetic moments of neutron-rich calcium isotopes (in contrast to previously derived  $pf$  shell

MBPT interactions [40]).

Finally, we comment briefly on the  $^{50}\text{Ca}(-1n)$  spectroscopic factor populating the  $^{49}\text{Ca}$  ground state, associated with removal of  $2p_{3/2}$  neutrons. Within an extreme single-particle description, a value of  $C^2S = 2$  is expected – both GXPF1 and the two NN+3N interactions exhaust >75% of this maximum value. Including the possible systematic error associated with overestimation of the ground state, as discussed above, the present measurement of  $2.7(\pm 0.4)_{stat}(\pm 0.5)_{sys}$  is slightly above 2, but agrees within errors. It is interesting to note that an apparent enhancement of  $l = 1$  and depletion of the  $l = 3$  strength was reported in the neighboring Sc isotopes [41].

In summary, first measurements of spectroscopic factors in  $^{50}\text{Ca}(-1n)$  that access wavefunction overlaps, considered together with recent electromagnetic properties, provide intriguing results on the shell evolution in the Ca isotopes beyond  $N=28$ , and point to the need of refining shell model interactions. Current state-of-the-art shell-model calculations make different predictions regarding the population of  $7/2_1^-$  states following direct neutron removal from  $^{48}\text{Ca}$  and  $^{50}\text{Ca}$ . The present results indicate a reduction of the strength populating the  $7/2_1^-$  state in  $^{49}\text{Ca}$  as compared to  $^{47}\text{Ca}$  outside of all model expectations. The best agreement is obtained with shell-model calculations based on NN+3N forces in the neutron  $pf$  model space, while the results are inconsistent with calculations using the phenomenological GXPF1 interaction, and with NN+3N calculations including the  $\nu 1g_{9/2}$  orbital.

The authors thank the operations team at NSCL for their work in beam delivery during the experiment. This material is based upon work supported by the U.S. Department of Energy, Office of Science, Office of Nuclear Physics under Contracts No. DE-AC02-05CH11231 (LBNL) and No. DE-AC02-06CH11357 (ANL), by the Department of Energy National Nuclear Security Administration under award number DE-NA0000979, the National Science Foundation (NSF) under PHY1102511, the European Research Council Grant No. 307986 STRONGINT and the BMBF under Contract No. 05P15RDFN1. HLC also acknowledges the U.S. DOE under grant No. DE-FG02-88ER40387 (OH). JAT acknowledges the support of the United Kingdom Science and Technology Facilities Council (STFC) under Grant No. ST/L005743/1. JM was supported by an International Research Fellowship from JSPS, and Grant-in-Aid for Scientific Research No. 26-04323. GRETINA was funded by the U.S. DOE Office of Science. Operation of the array at NSCL is supported by NSF under Cooperative Agreement PHY11-02511 (NSCL) and DOE under Grant No. DE-AC02-05CH11231 (LBNL). Computations were performed with computing resources at the Jülich Supercomputing Center.

- 
- [1] F. Wienholtz *et al.*, Nature **498**, 346 (2013).
  - [2] D. Steppenbeck *et al.*, Nature **502**, 207 (2013).
  - [3] J. D. Holt, T. Otsuka, A. Schwenk and T. Suzuki, J. Phys. G **39**, 085111 (2012).
  - [4] G. Hagen, M. Hjorth-Jensen, G. R. Jansen, R. Machleidt and T. Papenbrock, Phys. Rev. Lett. **109**, 032502 (2012).
  - [5] A. T. Gallant *et al.*, Phys. Rev. Lett. **109**, 032506 (2012).
  - [6] J. D. Holt, J. Menéndez and A. Schwenk, J. Phys. G **40**, 075105 (2013).
  - [7] G. Hagen, P. Hagen, H.-W. Hammer and L. Platter, Phys. Rev. Lett. **111**, 132501 (2013).
  - [8] V. Somà, A. Cipollone, C. Barbieri, P. Navrátil and T. Duguet, Phys. Rev. C **89**, 061301(R) (2014).
  - [9] S. Binder, J. Langhammer, A. Calci and R. Roth, Phys. Lett. B **736**, 119 (2014).
  - [10] J. D. Holt, J. Menéndez, J. Simonis and A. Schwenk, Phys. Rev. C **90**, 024312 (2014).
  - [11] H. Hergert, S. K. Bogner, T. D. Morris, S. Binder, A. Calci, J. Langhammer and R. Roth, Phys. Rev. C **90**, 041302(R) (2014).
  - [12] K. Hebeler, J. D. Holt, J. Menéndez and A. Schwenk, Annu. Rev. Nucl. Part. Sci. **65**, 457 (2015).
  - [13] G. Hagen *et al.*, Nature Physics **12**, 186 (2015).
  - [14] R. F. Garcia Ruiz *et al.*, Nature Physics **12**, 594 (2016).
  - [15] G. Hagen, G. R. Jansen and T. Papenbrock, arXiv:1605.01477.
  - [16] S. R. Stroberg, A. Calci, H. Hergert, J. D. Holt, S. K. Bogner, R. Roth and A. Schwenk, arXiv:1607.03229.
  - [17] J. Erler, N. Birge, M. Kortelainen, W. Nazarewicz, E. Olsen, A. M. Perhac and M. Stoitsov, Nature (London) **486**, 509 (2012).
  - [18] M. Honma, T. Otsuka, B. A. Brown and T. Mizusaki, Phys. Rev. C **65**, 061301(R) (2002).
  - [19] M. Honma, T. Otsuka, B. A. Brown and T. Mizusaki, Eur. Phys. J. A **25**, 499 (2005).
  - [20] S. Paschalis *et al.*, Nucl. Instrum. Methods Phys. Res. A **709**, 44 (2013).
  - [21] J. A. Tostevin and A. Gade, Phys. Rev. C **90**, 057602 (2014).
  - [22] A. Gade *et al.*, Phys. Rev. C **71**, 051301 (2005).
  - [23] D. Morrissey, B. Sherrill, M. Steiner, A. Stolz, and I. Wiedenhoever, Nucl. Instrum. Methods Phys. Res. B **204**, 90 (2003).
  - [24] D. Bazin, J. Caggiano, B. Sherrill, J. Yurkon and A. Zeller, Nucl. Instrum. Methods Phys. Res. B **204**, 629 (2003).
  - [25] L. Riley *et al.*, to be submitted (expected Nucl. Instrum. Methods Phys. Res. A)
  - [26] T. W. Burrows, Nucl. Data Sheets **108**, 923 (2007), and references therein.
  - [27] J. K. Smith, private communication.
  - [28] D. Montanari *et al.*, Phys. Lett. B **697**, 288 (2011).
  - [29] R. Broda, Acta Phys. Pol. B **32**, 2577 (2001).
  - [30] L. A. Riley *et al.*, Phys. Rev. C **93**, 044327 (2016).
  - [31] A. Mutschler *et al.*, Phys. Rev. C **93**, 034333 (2016).
  - [32] A. Gade, *et al.*, Phys. Rev. C **77**, 044306 (2008).
  - [33] P. Martin *et al.*, Nucl. Phys. A **185**, 465 (1972).
  - [34] M. E. Williams-Norton and R. Abegg, Nucl. Phys. A **291**, 429 (1977).

- [35] K. Hebeler, S. K. Bogner, R. J. Furnstahl, A. Nogga and A. Schwenk, *Phys. Rev. C* **83**, 031301 (2011).
- [36] J. Simonis, K. Hebeler, J. D. Holt, J. Menéndez and A. Schwenk, *Phys. Rev. C* **93**, 011302 (2016).
- [37] A. E. L. Dieperink and T. de Forest Jr., *Phys. Rev. C* **10**, 543 (1974).
- [38] A. Gade *et al.*, *Phys. Rev. C* **93**, 031601(R) (2016).
- [39] N. Tsunoda, K. Takayanagi, M. Hjorth-Jensen and T. Otsuka, *Phys. Rev. C* **89**, 024313 (2014).
- [40] R. F. Garcia Ruiz *et al.*, *Phys. Rev. C* **91**, 041304(R) (2015).
- [41] S. Schwertel *et al.*, *Eur. Phys. J. A* **48**, 191 (2012).